ELSEVIER

Colloids and Surfaces B: Biointerfaces 19 (2000) 397–405

COLLOIDS AND SURFACES B

www.elsevier.nl/locate/colsurfb

Tip friction — torsional spring constant determination

G. Bogdanovic [a,b], A. Meurk [a], M.W. Rutland [a,b,*]

[a] *Institute for Surface Chemistry, PO Box 5607 114 86 Stockholm, Sweden*
[b] *Department of Chemistry, Surface Chemistry, Royal Institute of Technology, 100 44 Stockholm, Sweden*

Abstract

A non-destructive technique is presented for verifying torsional spring constants used in lateral force microscopy. Various calibrations of the microscope are required and these are detailed. The technique produces reasonable values which tend to be larger than those predicted from considerations of the cantilever dimensions. The differences are discussed in terms of length corrections and particularly the uncertainty in the thickness of the cantilevers, which has an enormous effect on the values obtained through a priori calculations. Methods for inferring the thickness are discussed. Further, artefacts in conventional force measurements related to the experiments performed here are discussed.

Keywords: Lateral force microscopy (LFM); Atomic force microscope (AFM); Friction; Torsional spring constant; Cantilever

1. Introduction

The atomic force microscope (AFM) is increasingly being used in nanotribological applications [1], providing lateral contrast images or friction-load curves. Several papers have highlighted the difference between lateral forces and friction forces, i.e. the quantitative state of the measured deflection [2–5]. As opposed to normal force measurements, quantitative friction forces can only be obtained if the particular AFM used has been calibrated with respect to torsional bending of the cantilever. Such calibration methods preferably results in separation of an instrument-dependent constant and a cantilever torsional spring constant from the combined response [6–9], although other methods exists [10,11]. If the calibration constant relating the lateral voltage signal to a tilt angle of the probe has been found, the spring constants of the lever provide the final step before friction force measurements can successfully be achieved from evaluation of so-called friction loops.

However, determination of torsional spring constants has not progressed as much as for normal spring constants. Experimental methods like shift in resonant frequency with added mass, static deflection under load and evaluation of power spectrum of thermal noise [12–14] can all provide normal spring constants with 90% accuracy [15]. When it comes to experimental evaluation of torsional spring constants the only successful is the wedge calibration method [11]. Toikka et al. [16] attached a glass fibre to a V-shaped lever and measured the torque in con-

* Corresponding author.

0927-7765/00/$ - see front matter
PII: S0927-7765(00)00147-8

tact. Considering the low values obtained for the torsional spring constant, it is very likely their method yielded the fibre spring constant rather than the lever. Thus, the majority use calculations based on dimension and material properties [17,18] or finite element analysis methods [19,20]. Typically the best accuracy is given when a ratio between normal and lateral spring constants are used, where the normal spring constant has been calibrated with one of the procedures indicated above. Unfortunately, this still involves both dimension and material properties which for bilayer levers, e.g. gold-coated silicon nitride V-shaped levers, require both SEM-analysis and material moduli of the actual lever materials. The accuracy is better for diving board (rectangular) levers than V-shaped. Altogether, rectangular levers bend more uniformly with increasing load than V-shaped [21,22] and should be considered better for quantitative friction force measurements.

We present an experimental procedure for evaluation of torsional spring constants of any cantilever, regardless of size, shape, material or coating. This calibration method can be performed with any AFM and requires no additional devices, thus rendering a torsional spring constant in situ prior to friction measurements. We have used this procedure to evaluate three rectangular cantilevers of various length (Silicon MDT) and also assessed an artefact occurring when standard V-shaped levers are used in friction and normal force measurements.

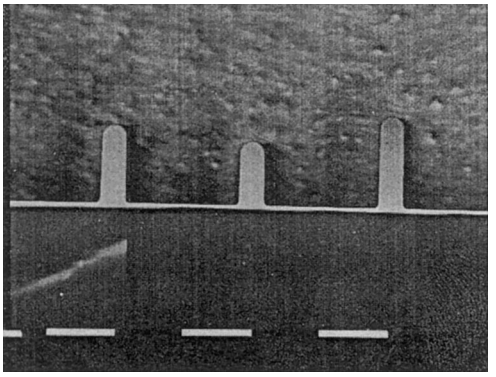

Fig. 1. SEM image showing the types of cantilevers calibrated for torsional spring constant. The cantilever on the left is referred to as A, the centre as B and that on the right as C. The cantilevers are Silicon MDT lateral force cantilevers, in this case without tips. The scale bar represents 100 μm.

2. Theory

While we present a general technique for measuring spring constants, we apply it here to rectangular beam cantilevers and so recapitulate the theory such cantilevers for later quantitative comparison with our measured results.

A rectangular lever of constant cross-section subjected to a moment M will twist an angle ϕ according to [7]

$$\phi = \frac{M}{GK} L \tag{1}$$

where G is the shear modulus and L the lever length. The polar moment of the cross-section, K, for a rectangular lever is

$$K = \frac{wt^3}{3} \tag{2}$$

where w is the lever width and t the lever thickness. The angle is thus described by

$$\phi = \frac{3FaL}{Gwt^3} \tag{3}$$

using $M = Fa$ where F is the applied load and a the distance associated with the moment.

The lateral spring constant k_ϕ (Nm/rad) is defined as

$$k_\phi = \frac{Gwt^3}{3L} \tag{4}$$

Combining Eqs. (3) and (4) gives

$$k_\phi \phi = Fa \tag{5}$$

which is the fundamental basic equation in this calibration procedure.

2.1. Experimental

Deflection measurements were obtained with a MultiMode NanoScope IIIa AFM (Digital Instruments, USA) in the force calibration mode. All cantilevers used were uncoated, tipless, rectangular silicon cantilevers of different lengths (Sili-

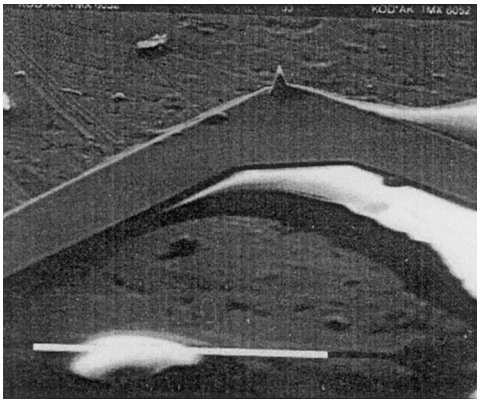

Fig. 2. SEM picture of lower surface assembly. A cantilever was glued with the sharp tip pointing upwards. The sharp tip is used to apply a turning moment to a cantilever mounted as usual in the AFM head. The scale bar represents 100 μm.

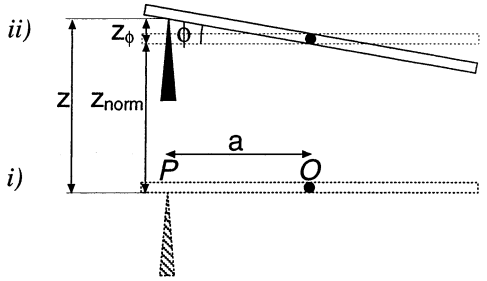

Fig. 3. Schematic of the experiment. When the cantilever is contacted by the tip mounted on the piezo, it responds with both normal and torsional deflections (if a is non zero).

con MDT, Russia), see Fig. 1. These levers are optimal for quantitative friction measurements due to high torsional bending linearity and ease of calculating the torsional spring constant from geometry and materials properties. Levers coated with gold or aluminium for increased reflectivity act as bimorphs and have shown to complicate the spring constant calculation [23,24]. The only complication arising from pure silicon levers is a larger tendency for laser interference to overlap the experimental data. This can, however, be compensated for experimentally. Normal spring constants of the cantilevers studied were determined by adding masses of known weights [12].

The substrate consisted of a tip-cantilever assembly turned upside down and glued to a silicon wafer (see Fig. 2). An epoxy resin (Araldite) hardening overnight was used for attaching the lever. Glue, tip and lever compliances were independently chosen not to influence the measured deflections, i.e. lever compliances dominated the contribution to the deflections. Acquisition of normal and lateral cantilever deflections were simultaneously done during an approach and retraction cycle, as performed during a force curve measurement.

2.2. Determination of frictional force constant

The technique developed here is applicable to any geometry of cantilever, though most conveniently to a rectangular beam. The tip glued to the surface is pointed upwards. It approaches the cantilever through an upward piezo scanner movement — in the z direction. All variables are defined as zero at first contact, of the tip on the lower surface with the cantilever case (i) in Fig. 3. The displacement of the lower surface, z, can be divided into two parts for the corresponding movement of the upper cantilever. The displacement of the centre O of the cross section, which is the distance z_{norm}, is the main part. z_{norm} is also referred to as the normal deflection of the cantilever. The second part, z_ϕ, is the additional displacement of the cantilever contact point P that results from the torsional angle ϕ of the cantilever. Assuming that the tip on the surface is rigid, we have by definition:

$$z = z_{\text{norm}} + z_\phi \tag{6}$$

where $z_\phi \ll z_{\text{norm}}$. The distance between the points O and P is a. For $a = 0$, where $z_{\text{norm}} = z$, the normal deflection voltage, V_z, is related to z_{norm} by the normal constant compliance slope:

$$C_z^0 = \frac{\Delta V_z}{\Delta z_{\text{norm}}} \tag{7}$$

For $a \neq 0$ we have

$$C_z^a = \frac{\Delta V_z}{\Delta z} \tag{8}$$

For the lateral (friction) voltage, V_ϕ, we define an angle detector constant as

$$\beta = \frac{\Delta V_\phi}{\Delta \phi} \tag{9}$$

and a torsional constant compliance slope as

$$C_\phi = \frac{\Delta V_\phi}{\Delta z} \tag{10}$$

The small angle approximation is valid for all measurements here so

$$z_\phi = a\phi \tag{11}$$

Eq. (5) in fact relates the moment M obtained from the torsional spring constant to the applied moment.

$$M = \phi k_\phi = F_\phi a \tag{12}$$

where F_ϕ is the force perpendicular to the cantilever surface. By definition the force experienced by the normal deflection of the cantilever must be the same as applied torsionally. allow us to put F_ϕ equal to the force $F_z = k_z z$, where k_z is the normal spring constant. From Eq. (12)

$$F_\phi = \frac{\phi k_\phi}{a} \tag{13}$$

that is

$$k_z z_{\text{norm}} = \frac{\phi k_\phi}{a} \tag{14}$$

Hence a plot of $k_z z/\phi$ against a^{-1} should give the torsional spring constant. Eq. (14) can be rewritten, replacing z_{norm} and ϕ with their respective voltages (Eqs. (7) and (9)) and rearranging slightly:

$$k_z\left(\frac{\Delta V_z}{\Delta V_\phi C_z^0}\right) = \frac{k_\phi}{\beta a} \tag{15}$$

The ratio V_z/V_ϕ is by definition the same as the ratio C_z^a/C_ϕ and the constant compliances are easily obtained from the raw data, thus an experimentally convenient form of Eq. (14) is

$$\frac{C_\phi C_z^0}{k_z C_z^a} = \frac{\beta}{k_\phi} a \tag{16}$$

where the gradient of the left hand side plotted against a gives the angle detector constant β, (which can be independently determined) normalised by the torsional spring constant.

Strictly, the parameter β can be simultaneously obtained from this treatment. Since

$$z - z_{\text{norm}} = z_\phi = a\phi \tag{17}$$

$$\Delta z - \frac{\Delta V_z}{C_z^0} = a\frac{\Delta V_\phi}{\beta} \tag{18}$$

$$\frac{\Delta z}{\Delta V_\phi} - \frac{\Delta V_z}{\Delta V_\phi C_z^0} = \frac{a}{\beta} \tag{19}$$

$$\frac{1}{C_\phi}\left(1 - \frac{C_z^a}{C_z^0}\right) = \frac{a}{\beta} \tag{20}$$

A plot of the left hand side vs. a will have a gradient of $1/\beta$. In practice, the torsional deflections are sufficiently small for C_z^a to be very close to C_z^0 so the bracketed term is very sensitive to small variations in C_z^a.

2.3. Scanner offset calibration

In order to experimentally evaluate the torsional spring constants, the distance a associated with the moment during torsional bending must be accurately determined. In between deflection measurements, the cantilever was moved perpendicular to the lever axis a certain distance using the offset command. Unfortunately, the piezo exhibits a strong nonlinearity in this function and apparent offsets can differ up to 30% to the actual offset distance moved. We thus calibrated our piezo with respect to the apparent offset and it displayed a typical quadratic dependence with an R^2 value of 0.9998. After calibration, the offset function was used to evaluate the lever width. This is a good test since width values are accurately controlled during microfabrication (in contrast to thickness) and hence rarely differ from the nominal value provided by the manufacturer. The $a = 0$ value was obtained through plotting the lateral constant compliance slope as a function of the offset position (the experimental measurement of a). The plot is a straight line, and the point at which the constant compliance is zero is then defined as $a = 0$. The applied load was obtained via the piezo movement and the spring constant. The former is calibrated regularly as a matter of routine using both interferometry and grids, the latter was measured by the resonance method.

2.3.1. Detector calibration

In surface force measurements the constant compliance region is routinely used for conversion of deflection data, assuming equal piezo movement and lever bending. However, care should be taken when the surfaces are coated with soft adsorbates, leading to an underestimation of both surface separation and interaction force [25]. In friction measurements the contact pressure is very high and substantial deformation of the surfaces involved occurs. Carpick et al. [26] and Lantz et al. [27] showed how shear strengths could be obtained from the initial surface deformations, i.e. energy dissipation, associated with friction measurements. Hence other contact independent methods are used for converting lateral deflections to friction force.

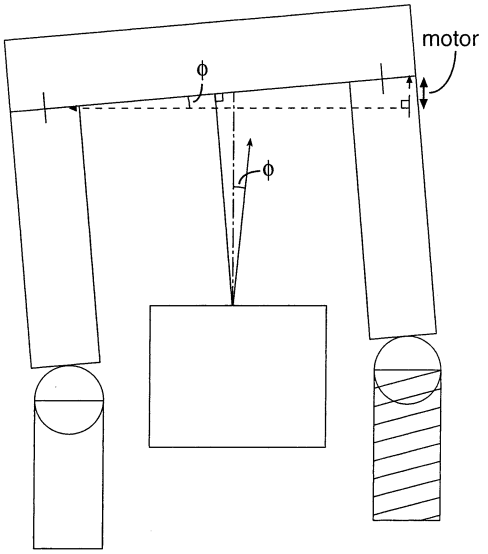

Fig. 4. Schematic of the technique used for calibrating the lateral deflection signal to obtain the constant β in Eq. (16). The angle of a mirror mounted beneath the head is altered using the head controls and the detector signal recorded.

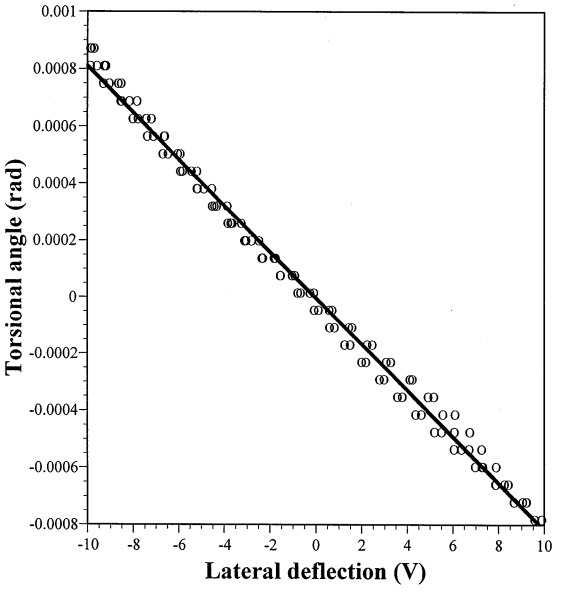

Fig. 5. Data from the angle detector constant determination according to the technique shown schematically in Fig. 4.

We calibrated the detector with respect to a torsional angle by using a mirror instead of a cantilever for reflection of the laser into the detector [9] (see Fig. 4). The lateral detector voltage was recorded as the mirror was tilted a certain angle with a stepper motor. A least squares fit to the data yields the conversion factor used for calculation of friction forces. Fig. 5 shows calibration results from an AFM. It is noteworthy that our second AFM, of the same type, gave a calibration factor which differed by a factor of four, which underscores the importance of calibrating individual AFMs used and not relying on reference values.

3. Results

The raw data appears as in Fig. 6. Note that rather than a 'voltage' being plotted on the vertical axis, we have used the instrumental units in which files are saved.

In the precontact regime of both traces an interferometric artefact is observed (the data has pronounced waviness rather than the preferred flat baseline). Since we are interested only in the contact regime, this artefact was ignored. It arises from the interference of the measurement beam deflected from the cantilever with light reflected from the lower substrate. As the lower surface moves, the relative path lengths of the two beams change, leading to an interference pattern of low amplitude, since the intensity of the scattered beam is much lower than that from the cantilever.

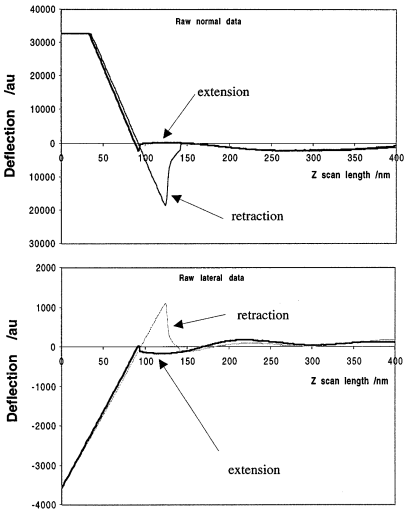

Fig. 6. Typical raw data. The normal and lateral deflections were simultaneously recorded as a function of the piezo expansion, z. The gradients of the constant compliance zones, where the surfaces are in contact, are a function of the experimental variable a, the distance from the longitudinal axis of the cantilever at which the force is applied. An interferometric artefact is observed in the non contact region.

We note that this property can be corrected for by adjusting the angle of the lower surface, and can be utilised to calibrate the piezo [28]. There is also slight hysteresis between the positions of the inward and outward runs (marked bolder and lighter respectively). This hysteresis is discussed extensively elsewhere [29] and need not concern us here.

As expected, the gradients of the constant compliance regions vary as a function of a, though this effect is not marked for the case of the normal deflection.

In Fig. 7 the constant compliances, obtained from data such as that shown in Fig. 6, are plotted according to Eq. (16) against a, the distance from the central axis at which the turning moment is applied.

As can be seen from the figure, the data in each case falls with reasonable accuracy along a straight line. The fitted line in each case has been constrained to pass through the origin and is a least squares fit. According to Eq. (16), the gradient of the line is the instrumental angular constant (in arbitrary units per radian) normalised by the torsional spring constant (in Nm/rad). The data has been shown in the figures in convenient units, the gradients have been converted to the more

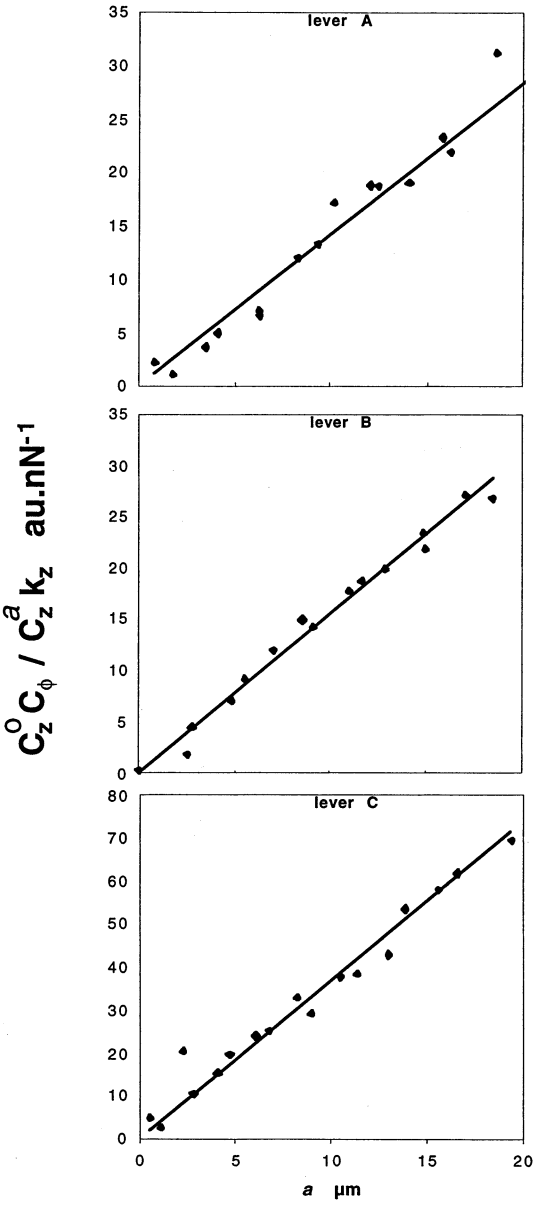

Fig. 7. Linearisation plots according to Eq. (16) for three different cantilevers; A, B and C. The lines are least squares fits, constrained to pass through the origin. The R^2 values range from 0.9839 for cantilever B to 0.9525 for cantilever A. The gradients are A 1.42 au.nN^{-1} μm^{-1}, B 1.56 au.nN^{-1} μm^{-1}, C 3.69 au.nN^{-1} μm^{-1}.

Table 1

Parameter	A[a]	B	C
k_ϕ measured (Nm rad^{-1})	2.80×10^{-8}	2.55×10^{-8}	1.08×10^{-8}
Length (μm)	113	87.1	130
Effective length (μm)	102	76	119
Thickness (μm)		Not measured	
Width (μm)	33.2	33.9	32.2
k_{norm} (N m^{-1}) (meas.)	1.1	2	0.69
Et^3 (Nm) (Eq. (21), meas. L, w)	1.41×10^{-7}	1.04×10^{-7}	1.44×10^{-7}
Effective thickness (μm)	0.99	0.90	1.00
k_ϕ calc using Et^3 above	5.87×10^{-9}	5.94×10^{-9}	5.01×10^{-9}
Length (μm)	**110**	**90**	**130**
Thickness (μm)	**1**	**1**	**1**
Width (μm)	**35**	**35**	**35**
k_{norm} (N m^{-1})	**0.7**	**1.7**	**0.6**
k_ϕ calc (Nm rad^{-1})	$\mathbf{5.91\times10^{-9}}$	$\mathbf{7.23\times10^{-9}}$	$\mathbf{5.00\times10^{-9}}$
k_ϕ meas/k_ϕ calc	4.73	3.53	2.16

[a] A, B and C refer to the three types of cantilevers shown in Fig. 1. The first row shows the result obtained for the lateral force constant by the technique presented here. In the next part of the table are the experimentally obtained values and quantities derived from them. For example, from the measured normal force constant, length and width a value for Et^3 can be obtained from Eq. (21) and this can be used to obtain an experimental thickness (using tabulated values for E) or an alternative value for the torsional spring constant. The value obtained in this way is higher than the value obtained from the manufacturers specifications (shown in bold in the table). Finally, the ratio of our experimentally obtained value to that of the calculated value is shown. This value is smallest for the longest cantilever.

fundamental units in Table 1 below. The magnitudes of the spring constants thus obtained are of the same order as the estimates obtained from the cantilever dimensions, which appears to validate the experimental approach. We estimate that all the experimentally obtained parameters in Eq. (16) are known with an accuracy of $\approx 1\%$, with the exception of the two spring constants. k_z can be obtained quite accurately through the resonance method [12] if enough added masses are used; in this case only two added masses were used per cantilever, giving a 'three point line'. We therefore pessimistically estimate the uncertainty in our measured normal spring constants to be 15%, and thus the uncertainty in our determined torsional spring constants is at most 15%.

3.1. Discussion

In all cases the measured spring constant is larger than the calculated one. There are probably several reasons for this. Firstly, our measurement is performed at the point on the cantilever immediately prior to tapering, so we are slightly underestimating the length in the experimental case. The point at which the measurement is made is approximately 11 μm from the end of the beam and therefore of the order of 5 μm from the position at which the tip would ordinarily be found. Secondly, the calculation assumes a uniform width which is not the case (Fig. 1). Most importantly, the calculations are based on manufacturer's specifications of the material properties and the cantilever thickness, a parameter which has cubic dependence in the equation. With the length correction, (of the order of 10% from Eq. (4)) the magnitudes can be made to match by assuming a cantilever thickness of 1.3 μm rather than 1.0 μm. This may conceivably explain the discrepancy, though the thickness is probably less than 1.3 μm as is seen below. For example it is likely that the reason that the spring constant obtained for cantilever B is smaller than that of cantilever A, contrary to the predicted order, is that there was a small thickness difference between the two chips. Note that A and C were

measured on the same chip, whereas B was from a second chip. Further evidence for the discrepancy being due to thickness variations is given by the fact that the normal spring constant as measured by the resonance technique [12] is uniformly larger than that quoted by the manufacturer, (see Table 1) despite the widths and lengths agreeing very closely. A reasonable explanation for this could be that the thickness differs from the quoted value. It is also interesting to note that this effect is largest for cantilever A which had the anomalously high value.

A value for the thickness of the cantilever can be 'tuned' by using the thickness as a fitting parameter in the dimensional equation for the normal spring constant, so that the calculation returns the value of the spring constant obtained from the resonance method (alternatively it can be used to obtain a value for Young's modulus if the thickness is known).

$$k_z = \frac{E\ w\ t^3}{4\ L^3} \tag{21}$$

The calculated thickness for A and C by this method are 0.99 and 1.00 μm whereas for cantilever B the thickness is 0.90 μm (using measured values of the length and width) Since A and C are from the same chip and the value of the measured torsional spring constant for A is greater than that for B, this estimate of the thickness certainly shows the right trend. It is also dependent on the value of Young's modulus.

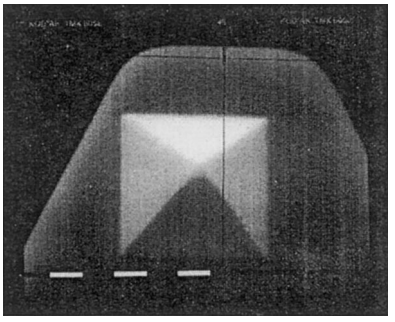

Fig. 8. SEM image of a V-shaped cantilever silicon nitride where the tip is not on the longitudinal axis of the cantilever, giving rise to torsional bending during normal deflection. The scale bar represents 1 μm.

The technique used here has an uncertainty of at most 15% and requires no knowledge of the cantilever thickness or material properties. The discrepancy between our measurements and calculations/quoted values can only be rationalised by invoking either different thicknesses or different material properties to those specified (or both). Thus the measured values are expected to be more reliable than calculated.

We also comment that the spring constants obtained by the resonance technique strictly ought to be divided by the cosine of the angle of tilt of the cantilever. This then gives the spring stiffness in the direction of motion of the piezo. In the present case this is $\approx 2\%$ correction and has been ignored.

In certain cases the placement of the tip is off centre as seen in Fig. 8 which can therefore lead to artefacts. This situation is exactly analogous to the situation we contrive in our experiments in Fig. 3. In this case the tip is on the cantilever rather than the lower surface and a is the distance off axis. Clearly, in response to movement of the lower piezo, there will be torsional deflection in contact giving rise to an apparent frictional force even when no sliding movement of the piezo is applied. In extreme cases it may also affect force measurements since the constant compliance in contact is used to determine the cantilever deflection, and it is assumed that the normal deflection of the cantilever is the same as the expansion of the piezo. If there is also torsional deflection this is not the case (Eq. (6)), though we have seen that at least for those cantilevers used here the z movement associated with torsional movement is small compared to the normal deflection due to the relatively higher spring constant. In our measurements, for the largest a values the torsional component of z did not exceed 10% of the total. In colloidal probe measurements however, care must therefore be taken to place the particles axially on the cantilever since the 10% error in measured force which could conceivably occur might affect parameters inferred from force measurement quite dramatically, such as surface potential, as well as making it difficult to get reproducible results. A simple and useful in situ

check of particle alignment is thus to monitor lateral deflection simultaneously.

4. Conclusion

Precise torsional spring constants have been successfully determined through this method. While the technique is rather laborious for routine calibration of cantilevers it further underscores how much caution needs to be used in applying literature or calculated values for frictional forces since these can deviate significantly from the measured values due to their sensitive dependence on thickness which is poorly controlled. In the method presented here the limiting factor in terms of precision is the normal spring constant, which if carefully evaluated can be determined to within 5%.

Design artefacts in tip design and off-centre gluing of colloidal probes could lead to spurious lateral deflection during normal force measurement, and possibly even lateral movement of the surfaces.

Acknowledgements

GB gratefully acknowledges funding provided by FPIRC (Forest Products Industry Research College) and AM's work performed within 'The Brinell Centre-Inorganic Interfacial Engineering', supported by the Swedish National Board for Industrial and Technical Development (NUTEK) and the following industrial partners: Erasteel Kloster AB, Höganäs AB, Kanthal AB, Sandvik AB, Seco Tools AB and Uniroc AB.

References

[1] B. Bhushan, Handbook of Micro/Nanotribology, CRC Press, Boca Raton, FL, 1995.
[2] R.W. Carpick, N. Agrait, D.F. Ogletree, M. Salmeron, J. Vac. Sci. Technol. B 14 (1996) 1289–1295.
[3] C.T. Gibson, G.S. Watson, S. Myhra, Wear 213 (1997) 72–79.
[4] E. Meyer, R. Lüthi, L. Howald, et al., in: H.-J. Güntherodt (Ed.), Forces in Scanning Probe Methods, NATO-ASI Series, vol. 286, Kluwer Academic Publishers, 1995, p. 285.
[5] M. Fujihara, in: B. Bhushan (Ed.), Micro/Nanaotribology and its Applications, NATO ASI Series, vol. 330, Kluwer Academic Publishers, 1997, p. 239.
[6] O. Marti, Phys. Scripta T49B (1993) 599–604.
[7] E. Liu, B. Blanpain, J.P. Celis, Wear 192 (1996) 141–150.
[8] C.A.J. Putman, V. Igarashi, R. Kaneko, Appl. Phys. Lett. 66 (1995) 3221–3223.
[9] A. Meurk, I. Larson, L. Bergström, Mat. Res. Symp. Proc. 522 (1998) 427.
[10] R.J. Warmack, X.Y. Zheng, T. Thundat, D.P. Allison, Rev. Sci. Inst. 65 (1994) 394–399.
[11] D.F. Ogletree, R.W. Carpick, M. Salmeron, Rev. Sci. Inst. 67 (1996) 3298–3306.
[12] J.P. Cleveland, S. Manne, D. Bocek, P.K. Hansma, Rev. Sci. Inst. 64 (1993) 403–405.
[13] T.J. Senden, W.A. Ducker, Langmuir 10 (1994) 1003–1004.
[14] J.L. Hutter, J. Bechhoefer, Rev. Sci. Inst. 64 (1993) 1868–1873.
[15] C.T. Gibson, G.S. Watson, S. Myhra, Nanotechnology 7 (1996) 259–262.
[16] G. Toikka, R.A. Hayes, J. Ralston, J. Adhes. Sci. Technol. 11 (1997) 1479–1489.
[17] J.M. Neumeister, W.A. Ducker, Rev. Sci. Inst. 65 (1994) 2527–2531.
[18] A. Noy, C.D. Frisbie, L.F. Rozsnyai, M.S. Wrighton, C.M. Lieber, J. Am. Chem. Soc. 117 (1995) 7943–7951.
[19] J. Hazel, V. Tsukruk, Pol. Prep. 37 (1996) 567.
[20] J. Hazel, V. Tsukruk, J. Trib. (1999) (in press).
[21] M. Labardi, M. Allegrini, M. Salerno, C. Frediani, C. Ascoli, App. Phys. A Mater. Sci. Process. 59 (1994) 3–10.
[22] Y. Mitsuya, Y. Ohshima, T. Nonogaki, Wear 211 (1997) 198–202.
[23] J.E. Sader, Rev. Sci. Inst. 66 (1995) 4583–4587.
[24] J.E. Sader, I. Larson, P. Mulvaney, L.R. White, Rev. Sci. Inst. 66 (1995) 3789–3798.
[25] K. Schillen, P.M. Claesson, M. Malmsten, P. Linse, C. Booth, J. Phys. Chem. B 101 (1997) 4238–4252.
[26] R.W. Carpick, N. Agrait, D.F. Ogletree, M. Salmeron, Langmuir 12 (1996) 3334–3340.
[27] M.A. Lantz, S.J. Oshea, A.C.F. Hoole, M.E. Welland, Appl. Phys. Lett. 70 (1997) 970–972.
[28] M. Jaschke, H. Butt, Rev. Sci. Inst. 66 (1995) 1258–1259.
[29] P. Attard, A. Carambassis, M.W. Rutland, Langmuir 15 (1998) 553–563.